Tomographic Estimation of Continuous Damage Evolution in Metals Under Straining

A. Cagnasso, A. Sawczuk

Laboratoire de Mécanique et d'Acoustique, C.N.R.S., B.P. 71, F-13402 Marseille Cedex 9, France

ABSTRACT

Tomographic scannings of permanently deformed alluminium specimens were made in order to evaluate the influence of plastic prestraining and deformation induced internal damage on local and global changes in the material density. Preliminary tests on pure alluminium specimens subjected to uniaxial, deformation controlled extension are reported. Measurements of the X-ray attenuation were made employing a medical equipment for the computerized axial tomography.

Changes in local densities as well as in histograms of the density in the scanned layer are established at various values of plastic elongation. Differencies in densitities observed with increasing uniaxial straining are indicated as regard to their values, histograms and standart deviations. Profiles of the local density variation with large plastic strains are presented.

Local densities are observed to increase with the axial extension of specimens and to have a larger scatter in comparison to undeformed specimens. Experiments inform as to applicability of the tomography in testing of deformed solids and indicate the necessary quantitative research.

1. Introduction

Tomographic scanning is widely used in medical diagnostics. The computerised axial tomography allows to establish local densities for specific elementary volumes of a material layer of well specified thickness. Differencies in densities allow to disclose presence of particular tissues within the surrounding ones, for example the presence of a tumor.

The tomography uses X-ray, very concentrated, beams. The irradiation damping within the material along a specific path, is recorded. The measured values constitute sums of the attenuation in elementary elements [1] . The elementary volume varies with the thickness of the scanned layer, the lowest volume being 1.5 mm^3. A computer program for solving the equations regarding unknown local densities as well as computerised visualisation of the density values and variations constitute an essential element of the testing method in question [2], [3].

The measurements are scaled in terms of Hounsfield units H. The unit corresponds to the X-ray attenuation of one promille per unit mass. In the case of water this corresponds to the volumetric density variation around 2.10^{-4} g/mm^3. With increasing coefficients of damping per unit mass the Hounsfield unit corresponds to larger values of the volumetric density change.

To tests the homogeneity of density for composite materials and plastics as well as to assess the influence of fatigue the method was already qualitatively used,[4-8] . We attempt to estimate the influence of deformation on the material deterioration in order to see how this deterioration can be estimated employing the computerised axial tomography. Our attention is concentrated on plastic deformations [9] and on deformation induced continuous damage.

Internal damage due to straining is nowadays studied within the continuum mechanics. The deterioration is usually described by a scalar parameter associated with the net area of the stress supporting surface [10] or with the deformation itself [11] , although micrographic measurements indicate that the internal damage has an oriented character. The resulting macroscopic behavior of a damaged solid is anisotropic [12] . Theories employing a scalar damage parameter can be justified by randomly distributed voids and their growth with the material straining [13] . The voids growth and possible closing of some of the voids or internal cracks should necessarily result in the density evolution with the material straining.

The present note concerns application of a non-destructive technique of tomography to the density measurements of metals subjected to plastic deformations. The tests made were intended to be qualitative only in order to be able to assess whether the method might be of any practical use when assessing the internal scalar damage growth or to evaluate the density appearing in the density hardening theories of inelastic mechanical material behavior.

Sec. 2 contains the information about mechanical tests in uniaxial straing. The next one concerns the tomographic scanning equipment used and the principles of the method in applications to more dense materials in comparison to those of medical interest.

Sec. 4 concerns scaling tests regarding the density variations due to a prescribed heating. Tomographic measurements for two types of allùminium alloys are presented in order to show the sensitivity of the technique. The results of scanning of a permanently deformed alluminium alloy are presented in the next Section. Histograms of the density variation are presented and compared with that concerning an undeformed material. Comparisons of the standart deviations of measured quantities show that the material homogeneity as regard to local densities decreases with permanent deformations.

In Sec. 6 the results of mechanical and tomographic tests are related. An increase of density of a flat specimen subjected to uniaxial tension is observed and related to the permanent axial elongation. The note concludes with remarks on applicability of the tomography to material testing, with a need for developing an equipment with a larger scale and appropriate computer softwares.

2. Mechanical tests

Pure aluminium A7, Pechiney Voreppe, specimens were worked out of a sheet. The original cross-section was $A_o = 1 \times 3 = 3\ cm^2$ and the initial length of the measured zone $L_o = 10$ cm, although the specimen was appropriately longer. The specimens were tempered in the temperature 400-420°C for 2 h 30' and left in air to attain the room temperature.

The specimens were subjected to uniform axial extensions in deformation controlled test using 100 kN Instron testing machine. The extension with a constant speed of 2 mm/min was terminated at $\Delta L/L_o = 0{,}55$ when developed neck was visible. The test specimens before and after extension are shown in Fig. 1. The final deformation was not uniform. In the upper half of 5 cm length the elongation $\Delta L/L_o = 0{,}46$, whereas in the part with a neck formed $\Delta L/L_o = 0{,}64$.

The geometry changes were measured in zones A and B, subjected eventually to tomographic scanning of 6 mm slices, as indicated in Fig. 2.

The specimens used exhibited a large ductility and a nonlinear load-extension diagram. In the plastic deformation range the load-deformation curve was almost parallel to the axis of extension, the specimen necking being observed beyond 40 % of elongation. The loading was stopped at 62 % of the maximal load.

3. Tomographic equipment

A medical scanner ND 8000 of French production by CGR was used. The scanner is designed and endowed with the software appropriate to tomography of brain. It employs X-ray tungsten tubes of power 480 W per mm^2 and Xenon receivers. The impulses of radiation consequently rotate by 12° to cover a full rotation. The tests in question were made on 6 mm slices.

The equipment used employs the current of 120 kV and assures a monochromatic radiation as the X-rays pass through a copper-gold filter LD3 of 1 mm. The energy of radiation used in 73 keV and the wave length 0,170 Å.

The principle of a scanner is to use X-rays of intensity I_o and to measure the intensity of radiation I after the passage of a beam through the material tested. The fundamental relation regarding these two quantities

$$I = I_o \exp\ (\mu_m \varrho\ x) \qquad (1)$$

where μ_m denotes the attenuation constant per unit mass of the material tested, ϱ stands for the volumetric density and x denotes the passage length of the beam through the material. The quantity $\mu_m \varrho = \mu\ [cm^{-1}]$ is used when endowing a scanner with a scale. This means that the coefficient of attenuation per unit length of the transversed material is employed. Once μ_m, I_o, I and the length of an attenuated beam are know the density ϱ can be calculated.

The attenuation constant $\mu = \mu_m$ for water is related to the zero value on the scale of damping, expressed in Hounsfield units H. The scale is such that the density of air is associated with − 1000 H and to the compact bone the attenuation value 1000 H is given. At the used tension and the emission energy $\mu = 0{,}19\ cm^{-1}$ for water.

For materials with larger μ than those met in living tissues the medical scale has to be appropriately modified. For example, in the case of an alluminium alloy of = 2.66g/mm^3, irradiated employing a tungsten tube at 120 kV and 73 keV, when 1 mm gold/copper filter is used, the wave length is 0.170 Å, $\mu_m = 0.233$, [14] . Then the coefficient of linear attenuation takes the value $\mu = 0{,}620 > 0{,}38\ cm^{-1}$. The number of Hounsfield units is therefore larger than H = 1000. We use the scale where zero corresponds to - 500 H in the medical one, whereas - 1000 H corresponds to the attenuation in air. The scanner used is adapted to such a scale change by an appropriate change in the solftware. By this modification in scale the sensitivity of tomographic data is changed and 1H does not correspond to $2.10^{-4}\ g/mm^3$.

4. Scaling tests

In order to get an information as to the possibility of utilisation of a medical scanner and the magnitude of density changes measured with the modified scale tests were made in the case of thermal expansion.

A cylinder 2R = 60 mm, L = 104 mm, of a commercial alluminium alloy AG3 was scanned at the temperatures 18°C and 110°C. The specimen was placed in a plaster tube therefore the numerical values of the Hounsfield units are not specifically significative. The purpose of the test consisted in comparing the values obtained at different volumes. For AG3 the density is $\rho = 2{,}66\ g/mm^3$ and the coefficient of linear thermal expansion $\beta = \frac{\Delta L}{L_0} = 0$ at 20°C. At 127°C $\beta = 0{,}259$ % and for the temperature 110°C we assume $\beta = 0{,}220$ %.

The volume after heating, neglecting second order terms is $V = \pi R^2 L\ (1 + 3\beta)$. Hence the volume increase due to heating is $\Delta V/V = 3\beta = 0.66$ %.

Hence the density decrease becomes $\Delta\rho = -3\rho\beta = 0{,}017\ g/mm^3$.

The values and histograms of the densities measured are given in Fig. 3 expressed in the H-units in the scale used. The densities are correspondingly $\rho = 2{,}660\ g/mm^3$ at 18°C and $\rho = 2.643\ g/mm^3$ at 110°C. 1 H means about $1{,}7.10^{-3}\ g/mm^3$.

To compare the alloys of different densities test were made cylinder of the same shape and dimensions at the room temperature. For AG3 is $\rho = 2.660\ g/mm^3$ and $\rho = 2.702\ g/mm^3$ for A5. The difference measured was 29H. Hence $1H = 1.4.10^{-3}\ g/mm^3$, thus of the order of that obtained in more specific tests on the same heated material.

5. Tomographic tests at plastic strain

The tests were made in zones A and B, close to the end of the deformed part and to the neck, as indicated in Fig. 2. The slices of 6 mm were scanned.

In Fig. 4 the histogram of an undeformed specimen of the used alloy is shown as visualised on the screen for a restitution perpendicular to the scanned slices. The material is seen to be quite homogeneous as the shade of the picture practically does not vary. The density in the marked zone is 615 H.

In the deformed specimen we consider first the zone A, where deformation is quite uniform and of the order of 40 to 45 %. In Fig. 5 histograms of densities in slices A, D and F specified in Fig. 2, are given. It is seen that with the increasing deformation a shift toward larger values of H takes place and the material slices become less homogeneous as histograms are less steep and have a larger standart deviation.

Distribution of the local densities is shown in Fig. 6. The left hand side gives the density profile along the line ab. The axial strain varies but slightly from a to b but the densities are different in comparison to that of an undeformed specimen, Fig. 4. In Fig. 6b the density variation with the specimen width in the slice D is shown. An edge effect is observed and an increase of density in the middle of cross-section.

For the zone B in vicinity of the neck the axial deformation is non-uniform and the strain state triaxial with compressive transverse stress and strain. These quantities were not measured in the preliminary test reported on. In Fig. 7 the recorded density distribution in the layer 1, Fig. 2, is shown. The histogram shows that the density distribution differs significantly from that of an undeformed specimen as given in Fig. 4. To outline this difference in Fig. 8 comparisons of histograms is given and the respective recorded densities are marked, similarly as for zone A in Fig. 5.

In Fig. 9 the local density profiles are shown. The left hand side figure corresponds to the longitudinal section cd. It is seem that in comparison with Fig. 6, related to quite uniform strain the scanner data, show a greater difference as the axial strain increases. Within the layer, already close to the neck, the distribution of density varies as well, taking the larger value at the cross-section center. The different shades in the Fig. 9 correspond to distinct density ranges. The scanner allows to obtain appropriately quantified isodensity zones, thus to judge the density variation in the specimen. The isodensities are obtained on the basis of measurements, concerning adjacent slices scanned in sequence.

6. Comparison of tomographic and mechanical tests

Large plastic strains can be related to the tomographic data. In the present note the information is only indicative as the axial strain only was measured but in fact a combined stress and strain state develops in the specimen. In Fig. 10 the obtained densities, expressed in Hounsfield's units, are related to the axial extension. Knowing the deformation of the grid 5 x 5 mm traced before the mechanical test and the grid after the deformation the axial elongation could be evaluated.

In Fig. 11 the standart deviation is plotted against the axial elongation. The points marked correspond to the data recorded and illustrated in Figs 5 and 8. The scatter in standart deviation is quite pronounced. Nevertheless the fact that the internal changes and material deterioration are related to permanent strain can be remarked.

At a biaxial extension the measured densities will be different and will rather indicate the density decrease.

7. Conclusions

The presented tomographic measurements indicate that the scanning gives an information about the internal variation of material properties at plastic straining. The results are of informative character only and further tests should made at well defined strain states in order to be able to arrive at quantitative data and conclusions.

Medical scanners could presumably be efficiently used in assessing density changes of porous materials and in powder metal forming technology. For density hardening theories of soil behavior and at deterioration of rocks the method also seems to be worthwhile to apply. As the software of a medical scanner is specialized to density measurements in a very narrow range around the density of water it might be useful to develop a scanner for defined mechanical purposes. This would require an appropriate software.

It is to be remarked that although a density increase is observed at permanent deformations, geometric measurements of the deformed zone A indicate that there is no global volume change, in accordance with the standart assumption of the classical plasticity. In the necking zone Fig. 9 shows that an internal void developped.

One can conclude that even with a medical scanner qualitative research can be made with carefull measurements of the deformation state and on specimens following a well defined sequence of plastic deformations.

Acknowledgements. The Clinique Clairval in Marseille allowed us to use their tomographic equipment. This generosity is gratefully acknowledged. Advice of Professor H.J. LATIÈRE of the Laboratoire de Mécanique et d'Acoustique is deeply appreciated.

References

[1] HOUNSFIELD, G.N., "Computerised Transverse Axial Scanning (Tomography). Part. I Description of the System". British Journal of Radiology, 46, 1016-1022, (1973).

[2] SCHMIDT, R., "La tomodensitométrie assistée par ordinateur", Internal Report, Massion Phillips, Suresnes, (1978).

[3] KLAUSZ, R., "La tomodensitométrie à rayon X", 4ème Coll. Int. Méth. Contr. Nondestruct. (Grenoble 1979), Université de Grenoble, 103-107, (1979).

[4] TREMOLIERES, J., "La tomodensitométrie". Electronique Applications. N° 11, 41-47, (1979).

[5] LEFEVRE, H., "Utilisation industrielle de la tomodensitométrie", Echos CEA, Science et Technique, N° Spécial, 70-72, (1982).

[6] CAGNASSO, A., GAGNAGE, B., ROSELLO, R., SANTAMARIA, F., "Analyse et mesure des densités internes dans les matériaux non-métalliques" CRAS, Série B, 287, 219-221, (1978).

[7] CAGNASSO, A., JULIEN, Y., "Examen de l'état de fatigue statique et dynamique d'un matériau par tomodensitométrie". Rheol.Acta, 20, 511-516, (1981).

[8] CAGNASSO, A., LATIÈRE, H.J., "Tomodensitométrie de la zone fondue : alliages légers, matériaux thermoplastiques" in : Metallurgie de la zone fondue (Marseille 1981), Report 07, Soudure Autogène, Paris, (1981).

[9] HILL, R., "The Mathematical Theory Plasticity", Clarendon Press, Oxford, (1950).

[10] KACHANOV, L.M., "Time to Rupture under Conditions of Creep", (In Russian), Izv. AN SSSR, OTN, N° 8, 26-31, (1958).

[11] JANSON, J., HULT, J., "Fracture Mechanics and Damage Mechanics. A Combined Approach". J. Méc. Appl. 1, 69-84, (1977).

[12] LITEWKA, A., SAWCZUK, A., "Experimental Evaluation of the Overall Anisotropic Material Response at Continuous Damage", in : Drucker Anniversary Volume (Ed. J. Dvorak, R.T. Shield), Elsevier, Amsterdam (1983), (in press).

[13] JALINIER, J.M., "Mise en forme et endommagement". Thèse, Université de Metz, Metz (1981).

[14] KAELBIE, E.F. (Ed.) "Handbook of X-Rays" Mc Graw-Hill, New-York, (1967).

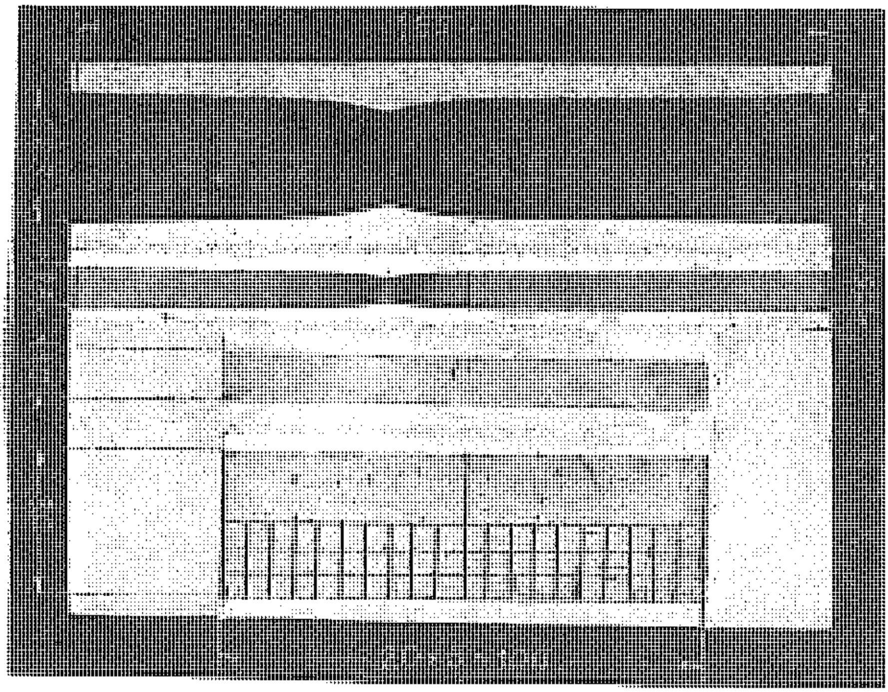

Fig. 1   Undeformed and deformed specimen

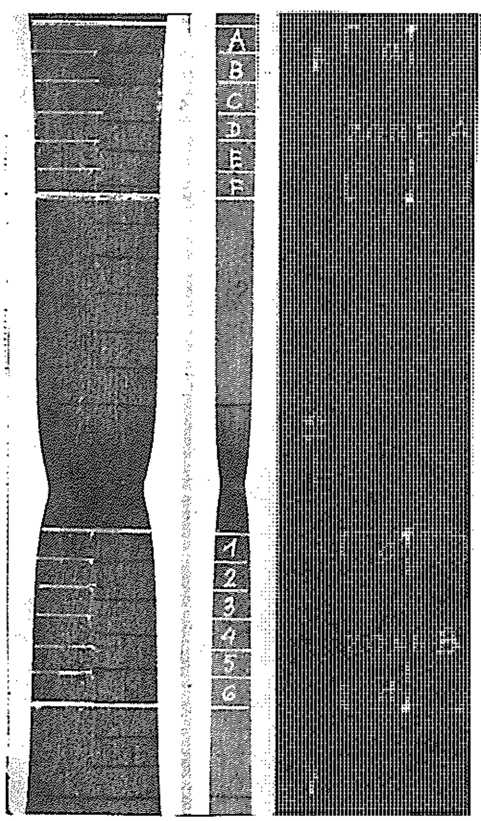

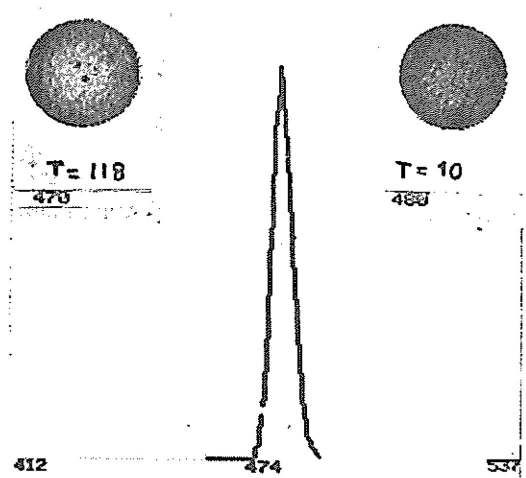

Fig. 3   Density variation with heating

Fig. 2   Scanned zones

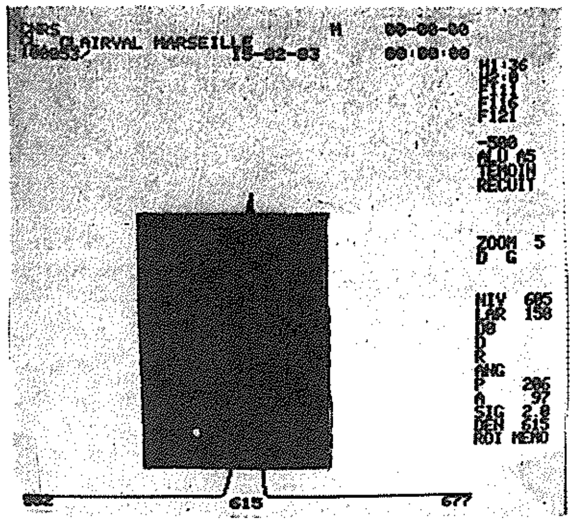

Fig. 4 Density distribution in an undeformed specimen

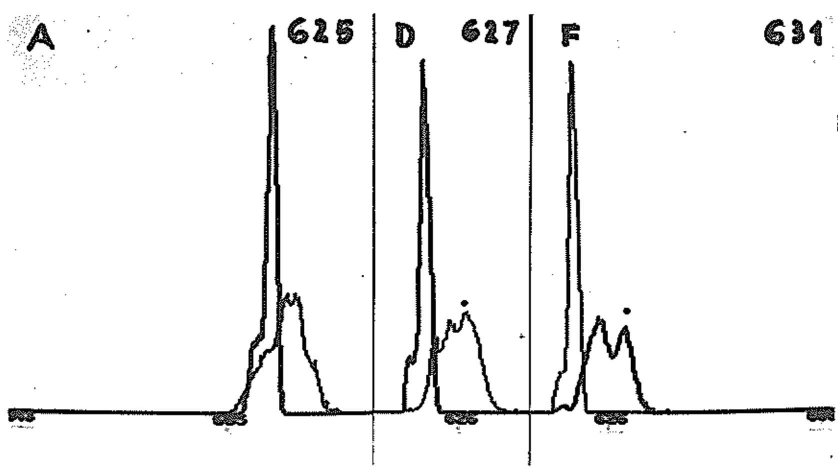

Fig. 5 Density changes and histograms at almost uniform plastic deformation

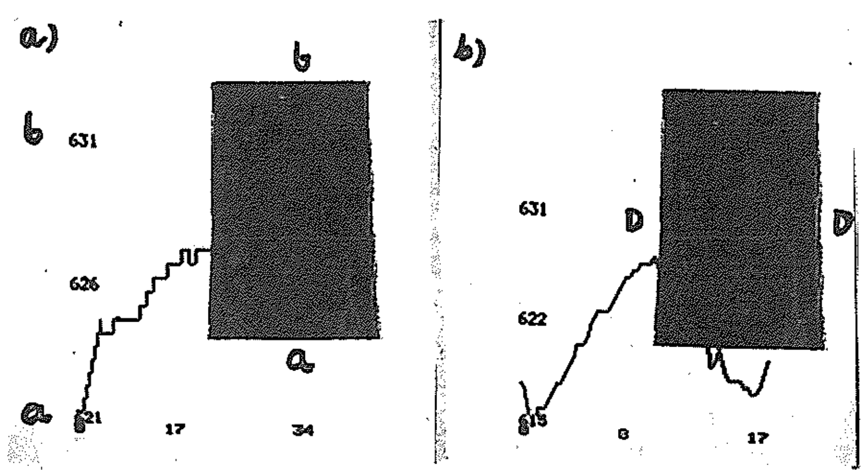

Fig. 6 Density profiles in zone A

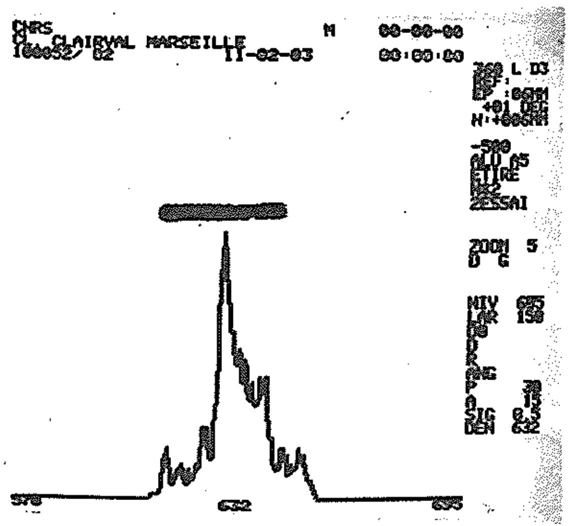

Fig. 7 Recorded density distribution in highly strained region of zone B

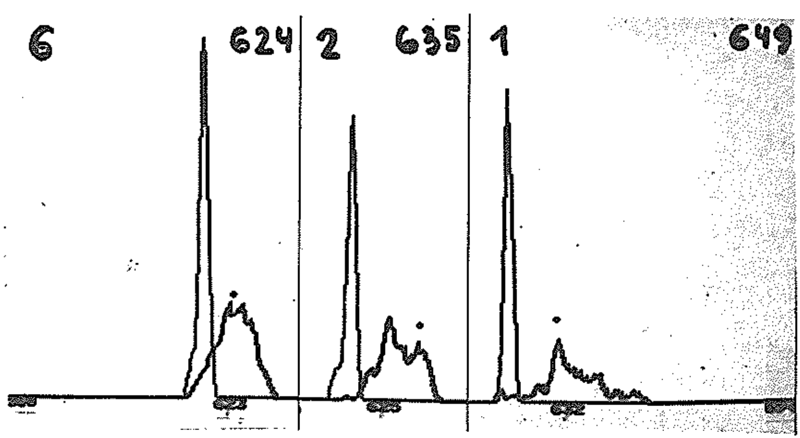

Fig. 8 Density changes and histograms at varying plastic deformation

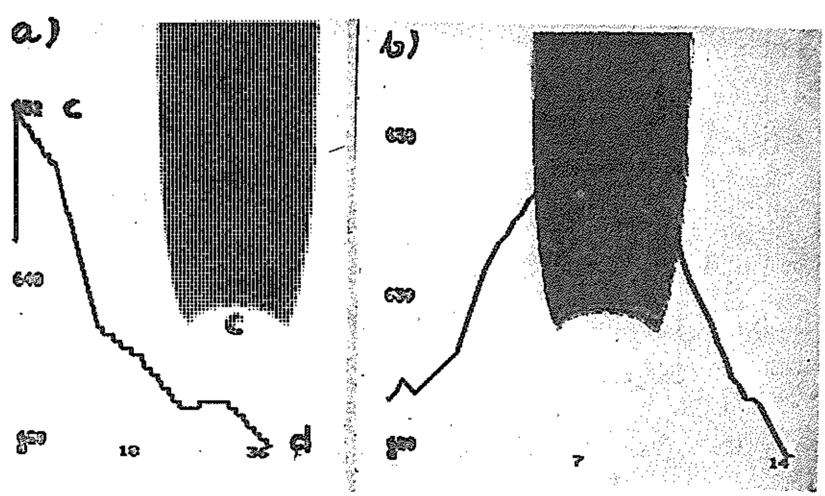

Fig. 9 Density profiles in zone B

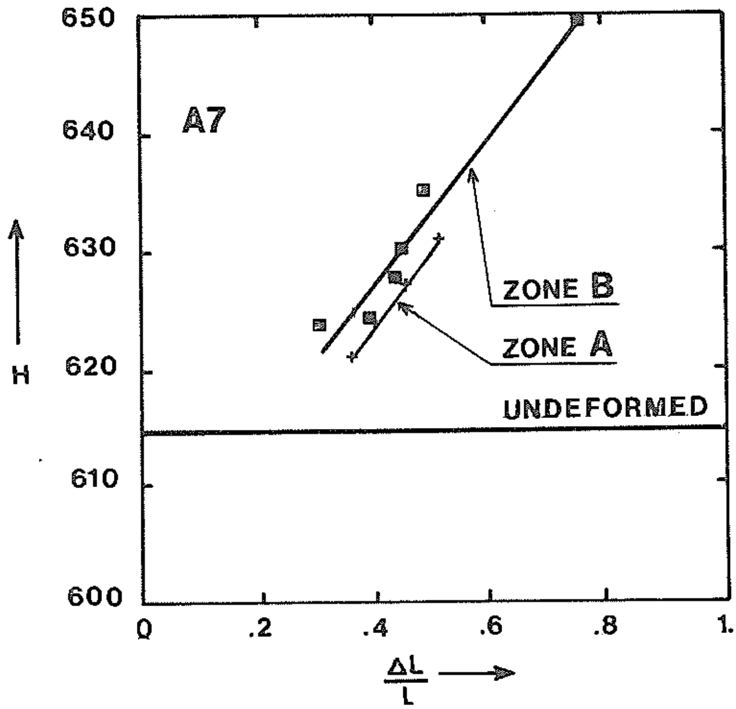

Fig.10 Density variation with permanent axial elongation

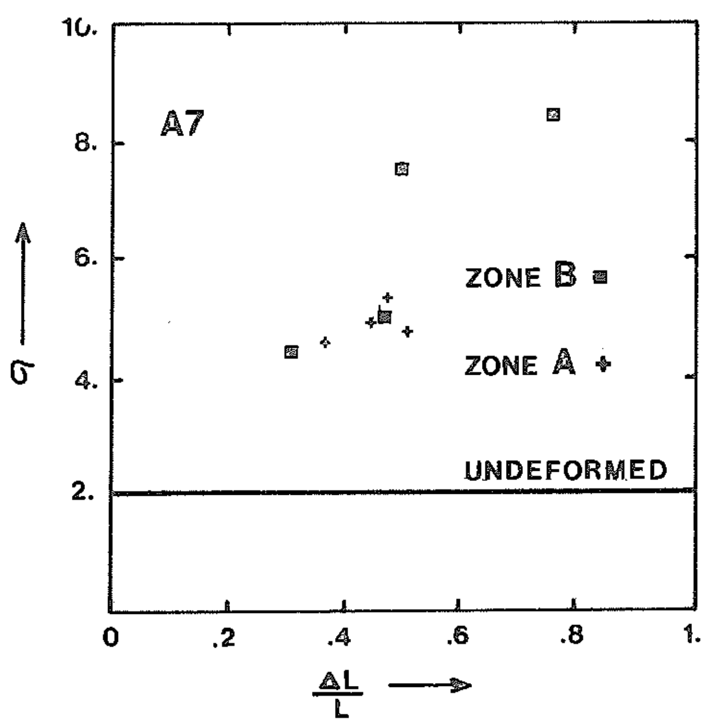

Fig.11 Standart deviation of density vs permanent axial elongation